INSTITUTE OF PHYSICS PUBLISHING JOURNAL OF PHYSICS B: ATOMIC, MOLECULAR AND OPTICAL PHYSICS

J. Phys. B: At. Mol. Opt. Phys. **34** (2001) 469–475 www.iop.org/Journals/jb PII: S0953-4075(01)17355-4

Studies of charge exchange in symmetric ion–ion collisions

C Y Chen[1], C L Cocke, J P Giese[2], F Melchert[3], I Reiser, M Stöckli, E Sidky and C D Lin

J R Macdonald Laboratory, Kansas State University, Manhattan, KS 66506, USA

Received 21 September 2000, in final form 15 November 2000

Abstract

We have measured the total cross sections for single charge exchange in He^{2+}–He^{+}, Ne^{2+}–Ne^{+} and Ar^{2+}–Ar^{+} collisions at centre-of-mass energies of 1.8–14.8, 1.8–10.8 and 2.8–7.3 keV, respectively, using an intersecting beam technique. The results for He^{2+}–He^{+} collisions are compared with existing measurements and calculations. For Ne^{2+}–Ne^{+} and Ar^{2+}–Ar^{+} the measured cross sections are compared with results from new close-coupling calculations based on a one-electron model potential description of the collision system.

1. Introduction

Theoretical calculations of total cross sections for resonant single charge transfer in symmetric ion–ion collisions have been carried out for several collision systems. These include (H^{+}–H)-like (Tharamel *et al* 1994), (Li^{+}–Li)-like (Tharamel *et al* 1994) and (Na^{+}–Na)-like (Bardsley *et al* 1989) systems. Experimental data for symmetric charge exchange between ions exist only for He^{2+} on He^{+}. Because of its simplicity and fundamental nature, this collision system has drawn much attention in both theory (Bates and Boyd 1962, Dickinson and Hardie 1979, Falcon 1983, Forster *et al* 1988, Bardsley *et al* 1989, Tharamel *et al* 1994) and experiment (Melchert *et al* 1992, 1995, Peart and Dolder 1979, Jognaux *et al* 1978). The single-charge-exchange cross sections for He^{2+}–He^{+} collisions from different theoretical calculations are found to be in good agreement with each other, but they were in disagreement with early measurements. However, they are in good agreement with the recent measurements of Melchert *et al* (1995) for centre-of-mass collision energies ranging from 200 keV down to 4 keV. In this paper we extend these measurements down to a centre-of-mass energy of 1.8 keV. In addition, we report cross sections for single charge exchange in the symmetric Ne^{2+}–Ne^{+} and Ar^{2+}–Ar^{+} collisions. (Centre-of-mass energies given in this paper refer to the homonuclear ^{4}He–^{4}He, ^{20}Ne–^{20}Ne or ^{40}Ar–^{40}Ar systems.)

[1] Present address: Institute of Earth Sciences, Academia Sinica, PO Box 1-55, Nankang, Taipei, 11529, Taiwan, Republic of China.

[2] Deceased July 1995.

[3] Permanent address: Physikalisch-Technische Bundesanstalt, Bundesallee 100, D-38116 Braunschweig, Germany.

0953-4075/01/030469+07$30.00

Table 1. Experimental parameters for He^{2+}–He^{+} collisions.

E_{cm} (keV)	$E_{He^{2+}}$ (keV)	$E_{He^{+}}$ (keV)	$V_{retarding}$ (kV)	$I_{He^{2+}}$ (nA)	$I_{He^{+}}$ (nA)	He^{+} rate (cps nA^{-1})	He^{2+} rate (cps nA^{-1})	Time (s)
1.8	10	5.6	+4	5.0	24.2	500	132	52 955
4.8	10	5.6	+2	6.0	17.2	450	140	19 012
15.25	14	7.5	−3	9.2	24.0	1185	158	76 830

2. Experimental approach

A schematic drawing of our central collision region and the post-collision analysis system is shown in figure 1. The doubly charged ions were produced by a 5 GHz ECR ion source, and the singly charged ions were produced by a Penning ion source. Both ion beams had energies below 10 keV q^{-1}. After momentum analysis by two dipole magnets, these two primary beams intersected each other at 90° in the collision region. The overlap of the ion beams was measured by scanning, in the vertical direction, a horizontal single slit with an opening of 0.9 mm oriented at 45° with respect to both ion beams. In order to separate the ion–ion collision products from ions coming from background collisions, the collision region was maintained at a high retarding voltage ($V_{retarding}$). The design of the interaction region has been described in detail previously (Giese *et al* 1992). After leaving the collision region, the ion beams were momentum analysed by dipole magnets. The primary ion beams were collected in Faraday cups and their currents were digitized by current integrators and recorded with a computer. The product ion beams were further separated from the background by cylindrical parallel-plate electrostatic analysers. Only those charged particles which underwent charge-changing processes in the collision region followed the correct trajectories to the two-dimensional position-sensitive MCP detectors. The signals from the detectors were measured in time coincidence. Figure 2 shows a time-coincidence spectrum for He^{2+}–He^{+} collisions at $E_{cm} = 1.8$ keV.

To obtain the absolute cross sections we measured the absolute detection efficiencies of our MCP detectors *in situ* using the technique described by Savin *et al* (1995). The absolute detection efficiency of each of our MCP detectors was measured to be $(38.3 \pm 2.8)\%$. To illustrate the performance of our apparatus, we list in table 1 the experimental parameters and measurement times for three He^{2+}–He^{+} runs.

3. Results and discussion

The energy dependence of the measured total cross sections for He^{2+}–He^{+} is shown in figure 3. The error bars shown in this figure, and all data figures in this paper, are only relative and are dominated by the counting statistics. An additional error in absolute scale of 7.4%, due mainly to the possible error in the detector efficiency, is not included in these error bars. The results are in excellent agreement with those of Melchert *et al* in the overlap energy region. Our results extend to slightly lower energies, and are in good agreement with published theoretical calculations (Falcon 1983, Forster *et al* 1988, Bardsley *et al* 1989, Tharamel *et al* 1994). To simplify the figure, only the theoretical curve of Bardsley *et al* (1989) is shown. We plot the data versus relative velocity rather than centre-of-mass energy to avoid confusion associated with the use of different isotopes in different experiments.

Our measured total charge transfer cross sections for the Ne^{2+}–Ne^{+} and Ar^{2+}–Ar^{+} collisions are shown in figures 4 and 5, respectively. We are not aware of any theoretical

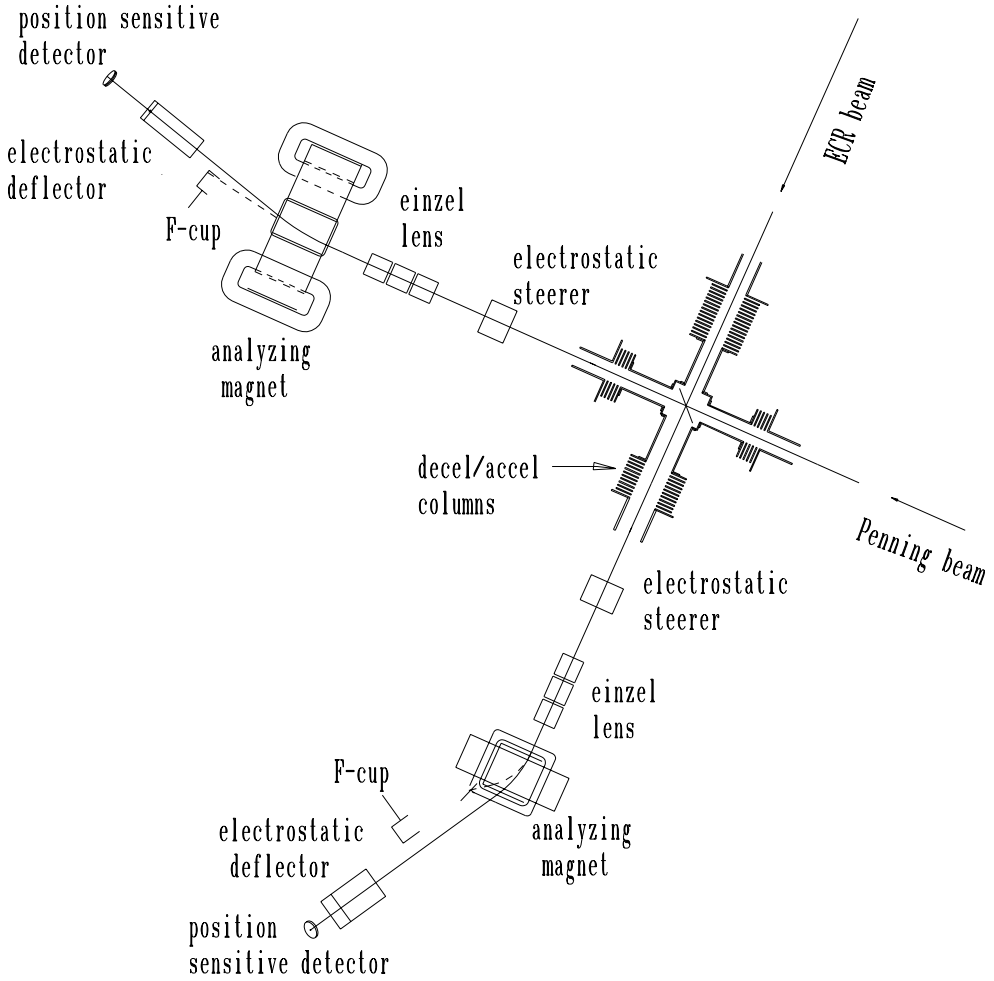

Figure 1. A schematic drawing of the KSU ion–ion collision facility.

calculations for these two symmetric collision systems. In order to compare with the measurements, we have performed a simple close-coupling calculation where we model the collision as consisting of one active electron only. Thus we model the collision of Ne^{2+}–Ne^{+} as a structureless Ne^{2+} ion impinging upon a target consisting of an electron initially attached to the Ne^{2+} 'bare' ion. The structureless Ne^{2+} is described by a model potential with parameters chosen such that it gives the correct binding energy of the 2p orbital of the Ne^{+} ion. For Ne^{2+}, the potential obtained is given by

$$V_{\mathrm{Ne}}(r) = \frac{-2 + (-8 + 2.2568r)\mathrm{e}^{-2.2568r}}{r}. \tag{1}$$

The binding energy for the 2p orbital obtained from this potential is 1.511 au, to be compared with the first ionization energy of Ne^{+}, which is 1.509 au.

Using this one-electron model, we calculated the charge transfer cross section for Ne^{2+}–Ne^{+}. The dominant process is the symmetric resonant charge transfer of the electron to the 2p state of the projectile Ne^{+}. In the close-coupling calculation using atomic orbitals as basis

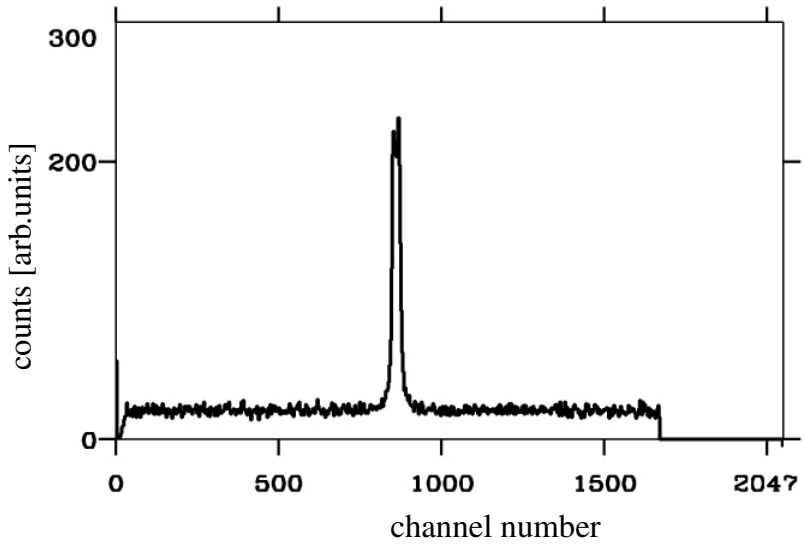

Figure 2. A time-coincidence spectrum for charge exchange for the collision system He^{2+} on He^{+} at $E_{cm} = 1.8$ keV. The time calibration is 1.18 ns/channel.

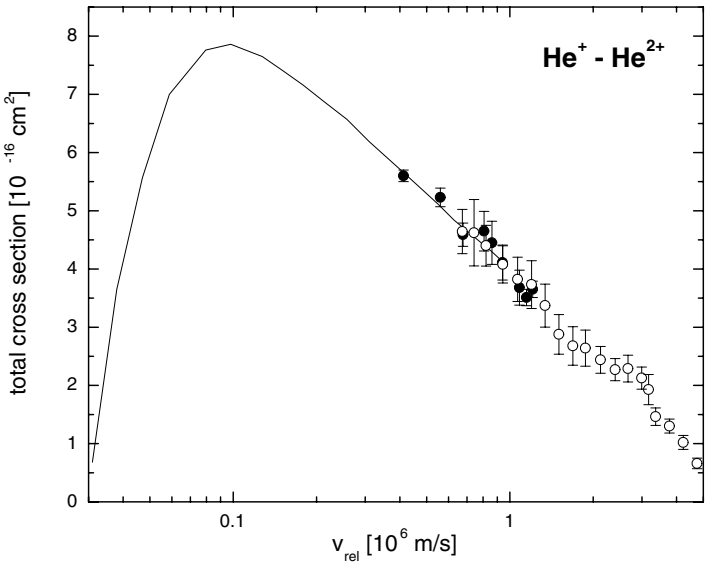

Figure 3. The total cross section for single charge exchange for He^{2+}–He^{+} collisions as a function of the relative velocity of the ions. ●, this experiment; ○, experiment by Melchert *et al* (1995); ——, theoretical calculation by Bardsley *et al* (1989).

functions (Fritsch and Lin 1991), we included all the magnetic substates of the 2p orbital on the target and on the projectile. Initially the electron is in one of the available magnetic substates. By solving the close-coupling equations (Fritsch and Lin 1991) total charge transfer cross sections were obtained. The reported theoretical charge transfer cross section is the result of averaging over the equally populated initial magnetic substates.

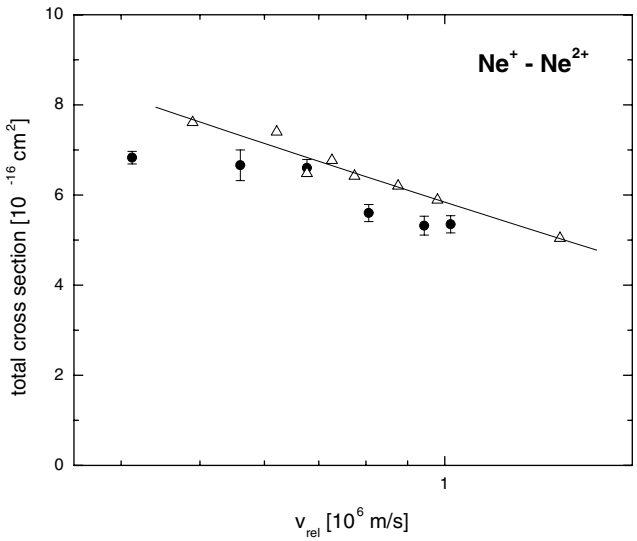

Figure 4. The total cross section for single charge exchange for Ne^{2+}–Ne^{+} collisions as a function of the relative velocity of the ions. ●, this experiment; ——, △, one-electron model calculation.

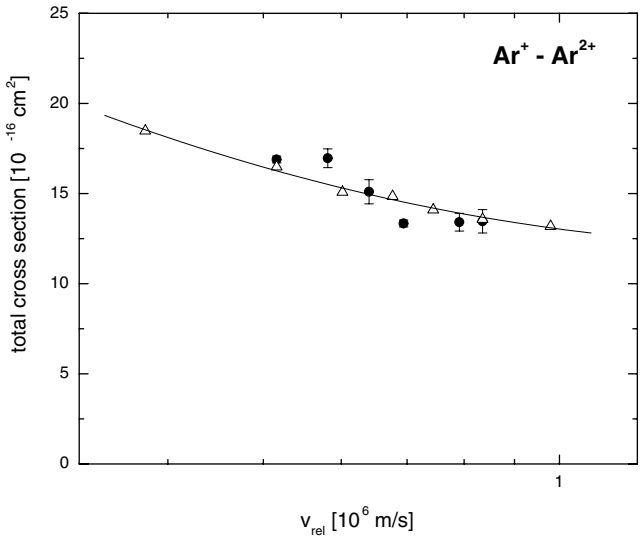

Figure 5. The total cross section for single charge exchange for Ar^{2+}–Ar^{+} collisions as a function of the relative velocity of the ions. ●, this experiment; ——, △, one-electron model calculation.

A similar model calculation was carried out for the Ar^{2+}–Ar^{+} collisions. The model potential used is

$$V_{\mathrm{Ar}}(r) = \frac{-2 + (-16 + 2.1703r)\mathrm{e}^{-2.1703r}}{r}. \tag{2}$$

This potential gives 1.016 au for the 3p binding energy, to be compared with the experimental ionization energy of 1.015 au.

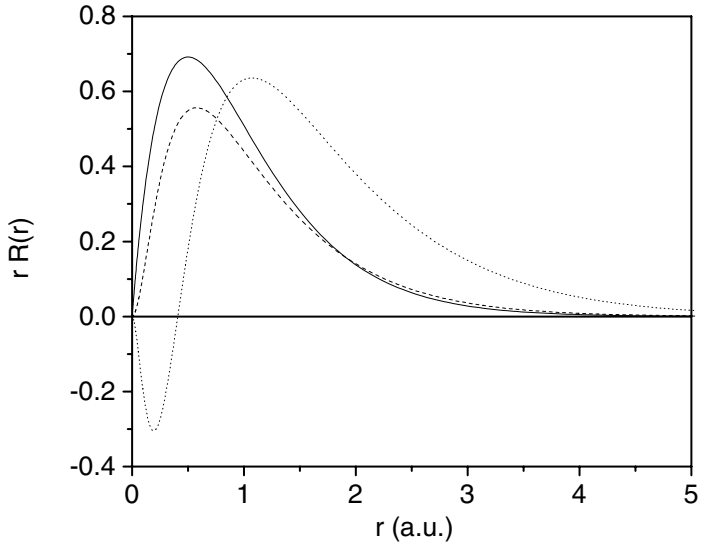

Figure 6. The r-weighted radial wavefunctions for $He^+(1s)$ (——), $Ne^+(2p)$ (– – –) and $Ar^+(3p)$ (· · ·) calculated as described in the text.

The results from this model calculation are shown in figures 4 and 5. They agree surprisingly well with the measured data, especially in view of the simplicity of the model for such complicated many-electron collision systems. There are small fluctuations with energy in the theoretical cross sections which are real within the model used, but which are unlikely to be physical. These structures can be traced to small variations with energy of the calculated transfer probabilities at small impact parameters, for which the model is least reliable. In order to draw the eye away from these fluctuations, we have drawn smooth curves through the calculated open triangles in figures 4 and 5.

The data show that the charge transfer cross section for He^{2+}–He^+ collisions is about the same as that for the Ne^{2+}–Ne^+ collision, while the cross section for the Ar^{2+}–Ar^+ collision in the same velocity region is about a factor of two larger. We have traced the origin of this result to be the size of the atomic orbital of the active electron involved in the collision. In figure 6 we show the r-weighted radial wavefunctions for $He^+(1s)$, $Ne^+(2p)$ and $Ar^+(3p)$ orbitals. For the last two systems, the wavefunctions are obtained from the model potentials above. It is interesting to note that the radial wavefunctions for $He^+(1s)$ and $Ne^+(2p)$ have essentially the same range, while the radial function of $Ar^+(3p)$ is further out. The longer 'tail' implies that the $Ar^+(3p)$ wavefunctions from the two centres begin to overlap at a larger internuclear separation. Such overlap is a necessary condition for the symmetric charge transfer to occur. Thus the larger size of the $Ar^+(3p)$ orbital explains the larger charge transfer cross sections. This qualitative interpretation is further supported by observing the calculated charge-transfer probabilities versus impact parameter. Over the energy range considered, the peak charge-transfer probability occurs at impact parameters near 2.8 au for the first two systems, but at 4.2 au for the last system. This difference in the range can account for almost a factor of two in the expected charge transfer cross section, in accord with the experimental measurements. We comment that the close-coupling calculations were carried out using straight-line trajectories, since the effect of Coulomb repulsion at the collision energies concerned is small.

It is perhaps surprising that the simple theoretical model employed here can reproduce the experimental data so well since several characteristics of the real collision system are not taken into account. The doubly ionized Ne or Ar system has multiplet structure which removes the degeneracy of the p^4 ($^3P^e$), $^1D^e$ and $^1S^e$ states by several eV. Thus the removal of a single p electron from the singly charged ion and addition of it to the doubly charged ion is not necessarily a resonant process. Furthermore, the Ne^{2+} and Ar^{2+} ions are produced in the beam with unknown fractions of metastable ions. Thus the Ne^{2+} projectiles are not necessarily in the $2p^4$ ($^3P^e$) ground state, but may also be in the metastable $^1D^e$ and $^1S^e$ states. The fractions of metastable ions may vary with the ion source conditions. We have varied the experimental ion source conditions in an attempt to alter the metastable fractions but were not able to change the experimental charge transfer cross sections.

The success of the simple model in the face of these complications may be due to the fact that the cross section is dominated primarily by the resonant symmetric charge transfer process, even if non-resonant channels are available as well. Test calculations carried out on these systems confirmed that removing the resonant nature of the collision greatly reduces the size of the calculated cross section. Thus it is likely that the non-resonant channels play little role in the collision. Even if the incident ion is initially in a metastable state, the symmetric charge transfer channel is still open and is still the dominant process. For the metastable ion, we expect its size to be comparable to that of the ion in the ground state. Since the symmetric charge transfer cross section is determined by the size of the radial function of the 'active' electron, the structure of the core plays little role. Thus the symmetric charge transfer cross section becomes independent of whether the core of the Ne^{2+} or Ar^{2+} is in the ground state or in a metastable state. If this interpretation is correct, one may expect more dependence of the observed cross section on the metastable fraction in the beam when asymmetric ion–ion collisions are studied.

Acknowledgments

This paper is supported by the Division of Chemical Sciences, Geosciences and Biosciences Division, Office of Basic Energy Sciences, Office of Science and the US Department of Energy. FM acknowledges support from the Alexander-von-Humboldt-Stiftung.

References

Bardsley J N, Gangopadhyay P and Penetrante B M 1989 *Phys. Rev.* A **40** 2742
Bates D R and Boyd A H 1962 *Proc. Phys. Soc.* **80** 1301
Dickinson A S and Hardie D W 1979 *J. Phys. B: At. Mol. Phys.* **12** 4147
Falcon C A 1983 *J. Phys. B: At. Mol. Phys.* **16** 1793
Forster C, Shingal R, Flower D R, Bransden B H and Dickinson A S 1988 *J. Phys. B: At. Mol. Opt. Phys.* **21** 3941
Fritsch W and Lin C D 1991 *Phys. Rep.* **202** 1
Giese J P, Chen C Y, Landers A, Stockli M, Richard P and Miller C 1992 *AIP Conf. Proc.* **274** 497
Jognaux A, Brouillard F and Szucs S 1978 *J. Phys. B: At. Mol. Phys.* **11** L669
Melchert F, Krudener S, Schulze R, Petri S, Pfaff S and Salzborn E 1995 *J. Phys. B: At. Mol. Opt. Phys.* **28** L355
Melchert F, Huber K, Krudener S, Schulze R, Meuser S, Pfaff S, Petri S, Benner M and Salzborn E 1992 *AIP Conf. Proc.* **274** 493
Peart B and Dolder K 1979 *J. Phys. B: At. Mol. Phys.* **12** 4155
Savin D W, Gardner L D, Reisenfeld D B, Young A R and Kohl J L 1995 *Rev. Sci. Instrum.* **66** 67
Tharamel J, Kharchenko V A and Dalgarno A 1994 *Phys. Rev.* A **50** 496